

BBA 77437

THE BINDING OF PHENOL RED TO RABBIT RENAL CORTEX

JILL EVELOFF*, WALTER K. MORISHIGE and SUK KI HONG**

Department of Physiology, University of Hawaii, School of Medicine, Honolulu, Hawaii 96822 (U.S.A.)

(Received February 24th, 1976)

SUMMARY

The binding of phenol red to the microsomal fraction of rabbit kidney cortex was rapid, reversible and consisted of two independent populations of binding sites: a high affinity and low capacity class which had an association constant of $11.29 \cdot 10^3 \text{ M}^{-1}$ and a binding capacity of $2.41 \mu\text{mol}$ phenol red bound per g of protein, and a low affinity binding population with an association constant of $0.80 \cdot 10^3 \text{ M}^{-1}$ and a maximal binding capacity of $55.06 \mu\text{mol}$ per g of protein. Probenecid (0.32 mM) competitively inhibited phenol red binding to only the high affinity binding site, whereas 2,4-dinitrophenol (0.77 mM) competitively inhibited phenol red binding to both the high and the low affinity population of binding sites. The binding of phenol red was highly sensitive to the cationic composition of the medium. The affinity of phenol red to the high and the low affinity binding populations was lowered by decreasing the sodium and potassium concentrations to 19 and 6 mequiv./l, respectively; however, the maximal binding capacity was unchanged. Calcium appeared to have no effect on the phenol red binding to the microsomes. All of these considerations suggest that the high affinity phenol red binding to the microsomal fraction may represent the interaction of phenol red with the physiological receptor necessary for organic acid transport at the peritubular membrane. Phenol red binding to the low affinity binding population may indicate an intracellular binding population which contributes to the intracellular accumulation of weak organic acids.

INTRODUCTION

The active step in weak organic acid secretion occurs at the peritubular membrane of the proximal tubule cells in mammals [1–3]. Supposedly, secretion is initiated by the binding of the weak organic acid to a carrier molecule within the peritubular membrane, forming a carrier-organic acid complex which is subsequently

* Present address: Mt. Desert Island Biological Laboratory, Salsbury Cove, Me. 04672, U.S.A.

** Present address: Department of Physiology, State University of New York at Buffalo, Buffalo, N.Y. 14214, U.S.A.

transported across the membrane where the organic acid is released into the intracellular space.

In mammals, intracellular accumulation occurs which has suggested to some investigators the presence of a binding component for weak organic acids within the cell [4–6]. The extent of weak organic acid binding to cellular constituents has never been satisfactorily examined. Two intracellular pools for *p*-aminohippurate are implicated from the kinetic treatment of influx and efflux data: a rapidly diffusible and equilibrating, probably free pool and a slowly diffusible bound pool [5–10]; however, the actual binding of *p*-aminohippurate to intracellular renal proteins has never been demonstrated [7, 11, 12]. The binding of *p*-aminohippurate has recently been investigated in dog renal cortical microsomes by Holohan et al. [11]. The binding was found to be temperature, time and pH dependent and subject to inhibition by probenecid and Diodrast. The binding of probenecid to rabbit renal cortical slices has been studied by Berndt [13] and was displaceable by bromocresol green. The microsomal binding of phenol red has been found to be inhibited by probenecid and 2,4-dinitrophenol, competitive inhibitors of phenol red secretion, by Sheikh [12], who postulated that the microsome is the cellular component where active, carrier-mediated secretion of phenol red occurs. However, no kinetic analysis of the data was done to verify the above hypothesis.

The present investigation was undertaken to study the nature of phenol red binding to various subcellular fractions of the rabbit kidney cortex, with the special reference to the kinetics of the specific binding of phenol red to the microsome.

MATERIALS AND METHODS

Tissue fractionation. Rabbits were sacrificed by an injection of air into the auricular vein. The kidneys were rapidly removed and perfused through the renal artery with ice-cold modified Cross-Taggart medium (90 mM NaCl, 40 mM KCl, 1.5 mM CaCl_2 , 10 mM Tris \cdot HCl, 10 mM sodium acetate, pH 7.4) to remove contaminating plasma proteins [14]. This Cross-Taggart medium was subsequently used as an incubation medium and buffer. Cortical slices were prepared with a Stadie-Riggs microtome and homogenized in 0.3 M sucrose (20 g/100 ml). The scheme used for tissue fractionation was similar to the method of de Duve et al. [15]. The crude homogenate was filtered through three layers of cheese cloth and centrifuged at $800 \times g$ for 10 min ($0-4^\circ\text{C}$). The sediment was washed once with 0.3 M sucrose. The pellet which contained nuclei as well as unbroken cells, was suspended in incubation medium to a final volume equal to four times the weight of the tissue processed (g/ml). The supernatants from the two $800 \times g$ centrifugations were combined and centrifuged at $16000 \times g$ for 15 min ($0-4^\circ\text{C}$). The pellet was washed once. The resulting mitochondrial pellet was resuspended in incubation medium equal to two times the original wet tissue weight. The microsomal fraction was isolated by combining the two mitochondrial supernatants and centrifuging for 1 h at $100000 \times g$ at $0-4^\circ\text{C}$. The resulting supernatant was termed the cytosol fraction. The microsomal fraction, which includes the plasma membranes of the cell [15], was routinely suspended in 4 ml of buffer to ensure enough sample for the binding analysis. Localization of the plasma membrane fraction was estimated by measuring the $(\text{Na}^+ + \text{K}^+)\text{-ATPase}$ activity as follows: 0.2 ml of the fraction was mixed with

0.6 ml of a solution containing 167 mM Tris · HCl buffer, 167 mM NaCl, 16.7 mM KCl, 5 mM MgCl₂ and 10^{-4} M ouabain (only in the case of ouabain inhibition). The reaction was initiated with the addition of 0.2 ml 15 mM ATP. ATPase activity was measured as μmol of P_i released/mg of protein, according to the method of Fiske and SubbaRow [16]. Approx. 90 % of the (Na⁺ + K⁺)-ATPase activity was consistently found in the microsomal fraction.

Binding reaction. The binding of phenol red to the subcellular fractions of the rabbit cortex was determined using ³H-labeled phenol red and employing centrifugation to separate the bound from the unbound dye. In general, 0.1 ml of ³H-labeled phenol red (0.04 μM) and 0.2 ml of Cross-Taggart buffer containing an appropriate concentration of unlabeled phenol red were added to the centrifuge tube. The binding reaction was initiated by the addition of 0.3 ml of the isolated fraction and conducted for 15 min at 25 °C. Incubation was terminated by centrifugation at a centrifugal force equal to that at which the fraction was isolated. The supernatant was withdrawn and the surface of the pellet was washed once with buffer. The binding of phenol red to the cytosol fraction was determined by precipitation of the cytosol proteins with 0.5 ml 20 % trichloroacetic acid after the incubation period, followed by centrifugation at $800 \times g$ for 10 min. This procedure was verified using equilibrium dialysis which gave identical cytosol binding data. The pellets were solubilized overnight with 0.1 ml of Protosol (New England Nuclear) and the activities of the pellet and the supernatant counted in Aquasol (New England Nuclear). The free phenol red concentration was calculated from the amount of ³H-labeled phenol red present in the supernatant. Radioactivity was measured with a Packard Tri-Carb spectrometer. A channels ratio method for quench correction was utilized.

Competitive or metabolic inhibitors of phenol red transport, when used, were added prior to the addition of the ³H-labeled phenol red. In studying the ionic requirements of phenol red binding, sodium-free buffer was prepared by substituting choline chloride equiosmotically for the NaCl. Potassium-free and calcium-free incubation mediums were also prepared substituting choline chloride equiosmotically for the chloride salt. The ³H-labeled phenol red was prepared in Cross-Taggart medium and therefore, when added to the cation-free media resulted in a final concentration of sodium, potassium and calcium of 19, 6.7 and 0.25 mequiv./l, respectively, during the ionic dependence studies.

The reversibility of phenol red binding was measured at a phenol red concentration of 0.01 μM . After 15 min of incubation when the binding of the labeled dye had reached a steady state, either 0.2 ml of Cross and Taggart buffer (control) or buffer containing various concentrations of unlabeled phenol red were added to the original 0.4 ml of incubation mixture. The tubes were vigorously shaken and reincubated for 15 min and the binding determined as previously described.

Subcellular distribution. The subcellular distribution of phenol red in renal cortical slices was studied after uptake into the slice. Approx. 300 mg of renal cortical slices were incubated in 10 ml of oxygenated buffer containing ³H-labeled phenol red and unlabeled phenol red for 1 h at 25 °C. Final phenol red concentrations were from 0 to 960 μM . At the end of the incubation period, the slices were removed from the buffer, blotted, weighed, fractionated as described previously, and assayed for ³H-labeled phenol red.

In order to investigate whether phenol red was metabolized within the renal

cortical slice, the dye was allowed to be taken up into the slice during a 1 h incubation period at 25 °C. The slice was homogenized to a 20 g/100 ml homogenate in ethanol and centrifuged at $800 \times g$, the supernatant applied to a Silica Gel-60 column (Merck) and eluted with water-saturated *n*-butanol. The phenol red was extracted from the homogenate with 0.1 M HCl in ethanol and the extract also passed through the column and collected in 0.5-ml samples. The elution patterns of the extracts were compared with that of a ^3H -labeled phenol red standard. All of the dye taken up into the slice eluted at an identical rate with the ^3H -labeled phenol red and therefore did not appear to be metabolized within the cortical slice.

All experiments were carried out on fractions prepared on the same day as the experiment. Protein was assayed by the method of Lowry et al. [17] using bovine serum albumin as a standard. In general, the binding data are expressed as μmol of phenol red bound per g of protein.

Reagents and radioactive compounds. Analytical grade reagents were used throughout the investigation. Uniformly tritiated phenol red was prepared by New England Nuclear Corp. to a specific activity of 5920 Ci/mol. The purity of the label was ascertained by column chromatography on silica gel - 60 (Merck) (column dimension = 13×240 mm), using water-saturated *n*-butanol as the mobile phase. All of the ^3H -labeled phenol red was quantitatively recovered in the elution volumes corresponding to the unlabeled authentic phenol red.

Statistical analysis. To evaluate whether statistical differences existed between the slopes of the corrected components of the Scatchard plot, a Student's *t*-test was employed where:

$$t = \frac{b_1 - b_2}{\sqrt{\frac{S_y \cdot x_1^2}{d.f._1} + \frac{S_y \cdot x_2^2}{d.f._2}} \cdot \sqrt{\frac{1}{\Sigma x_1^2} + \frac{1}{\Sigma x_2^2}}}$$

the slope is b , $S_y \cdot x^2$ is the mean square deviation from regression, Σx^2 is the sum of squares of the deviation and *d.f.* is the degree of freedom, which is the sample number minus 2.

RESULTS

Subcellular distribution of phenol red. The distribution of phenol red in the cortical cells was studied after the dye was taken up into rabbit renal cortical slices. The percentage of counts found in each fraction and the slice-to-medium ratio at the various phenol red concentrations are seen in Table I. The slice-to-medium ratio decreased exponentially with increasing phenol red concentrations and the slice-to-medium ratio curve employing ^3H -labeled phenol red was superimposable on curves using unlabeled phenol red alone. The cytosol fraction consistently contained the largest percentage (52 %) of the phenol red taken up into the slice, an expected result since in the slice preparation the tubular lumen are closed or blocked with debris. Thus to achieve increasing accumulation of dye against a concentration gradient, the dye must accumulate in the cytosol of the cell. Sheikh [12] also found 52 % of the phenol red in the cytosol of the cell after slice incubation.

Identification of the specific subcellular binding fraction. To determine which

fraction of the renal cortical cell specifically binds phenol red, the binding of phenol red to nuclear, mitochondrial, microsomal, and cytosol fractions was measured. The binding of phenol red to all of the subcellular fractions increased

TABLE I

PERCENT DISTRIBUTION OF PHENOL RED WITHIN THE RENAL CORTICAL CELL
Mean \pm S.E.; $n = 4$

Phenol red concentration (μ M)	Slice/medium	Nuclear	Mitochondrial	Microsomal	Cytosol
4	42.3 \pm 8.0	16.0 \pm 4.2	8.7 \pm 0.9	14.2 \pm 1.7	61.1 \pm 3.3
28.8	29.6 \pm 7.2	18.8 \pm 3.0	11.6 \pm 1.6	16.0 \pm 1.8	53.6 \pm 4.8
57.6	19.5 \pm 3.9	19.9 \pm 2.2	12.8 \pm 1.4	19.0 \pm 0.6	48.3 \pm 1.1
115.2	15.5 \pm 2.9	20.0 \pm 4.0	12.9 \pm 1.2	18.2 \pm 2.6	48.9 \pm 2.5
230.4	10.0 \pm 1.2	21.4 \pm 4.2	12.0 \pm 1.4	17.4 \pm 3.0	49.2 \pm 6.8
288	9.3 \pm 0.6	21.9 \pm 4.9	10.5 \pm 1.5	15.8 \pm 2.8	51.8 \pm 7.1
480	6.6 \pm 1.2	19.8 \pm 2.8	14.0 \pm 1.9	17.3 \pm 1.7	48.9 \pm 5.3
960	4.2 \pm 0.7	17.7 \pm 5.3	10.7 \pm 1.6	18.2 \pm 3.6	53.4 \pm 10.0
Average		19.4 \pm 3.8	11.7 \pm 1.4	17.0 \pm 2.9	51.9 \pm 5.1

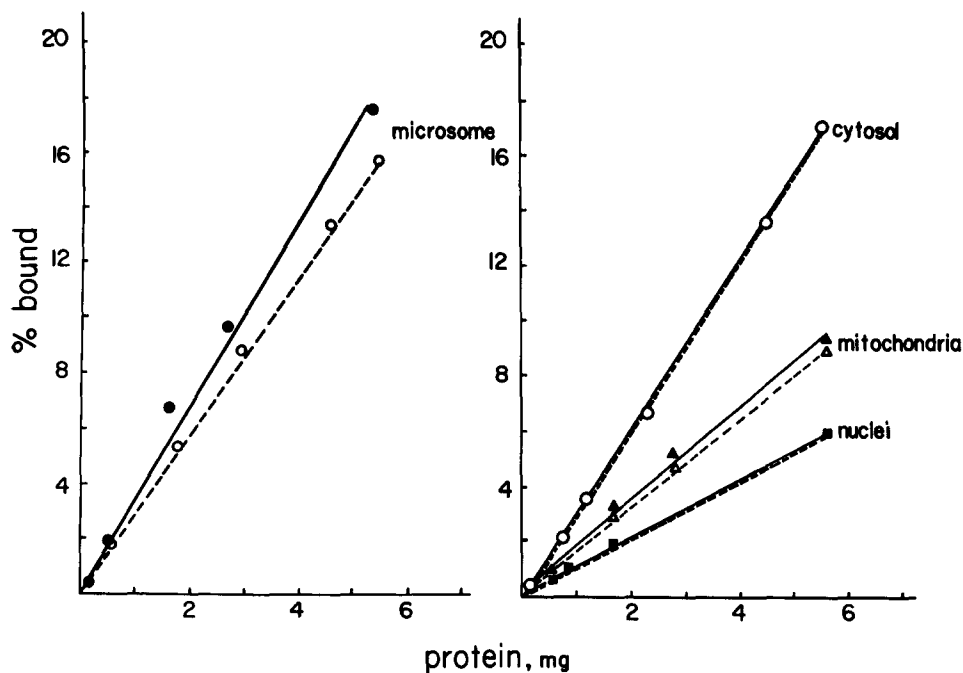


Fig. 1. The identification of the specific subcellular binding fraction for phenol red. The solid lines and circles (●—●) indicate the binding of the dye in the presence of 6.1 μ M phenol red. The dotted lines and open circles (○---○) are phenol red binding in the presence of 6.1 μ M phenol red plus 6.67 mM probenecid. Each point represents the mean of four experiments.

linearly over a range of 0.2–6 mg of protein (Fig. 1). Both microsomal and cytosol fractions had similar capacities for phenol red binding, approx. 18 % of the dose was bound at the higher protein concentrations. This value was 2-fold higher than that found for the nuclear and mitochondrial fractions, which bound approx. 9 % of the phenol red at an equivalent protein concentration. The addition of 6.67 mM probenecid decreased phenol red binding significantly only in the microsomal fraction ($p < 0.05$). This was taken as an indication that the microsomal fraction contained a competitively inhibitable binding component; therefore, the microsomal fraction was used throughout the rest of the study to characterize the phenol red binding process. The large magnitude of the cytosol binding component was unexpected and could be an important factor for the attainment of the high intracellular accumulation of weak organic acids seen in mammals.

Kinetics of binding to the microsomal fraction: time course of phenol red binding. The binding of phenol red to the microsomal fractions of the renal cortex was determined after incubation of the dye with the microsomal fraction for various lengths of time. The reaction was terminated by ultracentrifugation. This methodology does not produce a distinct endpoint for the binding reaction and was used as an estimate of the time necessary for the attainment of equilibrium of the binding reaction. As seen in Fig. 2, equilibrium levels were attained within 2 min of incubation followed by 1 h of centrifugation and no further increases were seen with 15 min or 1 h of incubation. Therefore, 15 min incubation periods were used throughout the binding experiments.

The time course for the reversal of phenol red binding was also rapid, and therefore, the association and dissociation rate constants could not be determined by the method employed in the present investigation.

Reversibility of phenol red binding. Phenol red binding was reversible as tested by experiments involving displacement of ^3H -labeled phenol red with increasing concentrations of unlabeled phenol red. After 15 min of incubation, when the binding of the labeled dye had reached a steady state, unlabeled phenol red in varying amounts

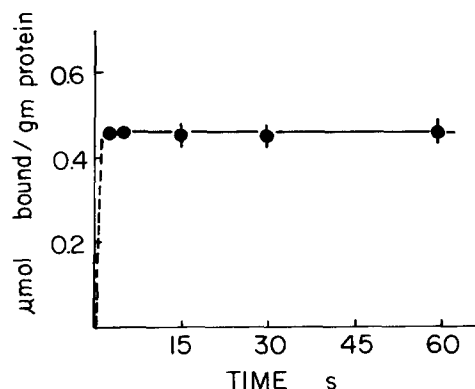


Fig. 2. The time course of binding of phenol red to the microsomal fraction of the renal cortex. The concentration of phenol red was $5.01 \mu\text{M}$. The dotted line represents the hypothetical time course of the binding reaction and the solid line, the determined time course. Points are means \pm S.E. ($n = 4$).

was added. The tubes were reincubated for 25 min. The bound ^3H -labeled phenol red was displaced by non-labeled phenol red (Fig. 3).

Relationship between phenol red concentration and binding. The effect of increasing phenol red concentrations on the binding of the dye to the microsomal fraction is seen in Fig. 4. Deviation of the binding plot from linearity suggests satura-

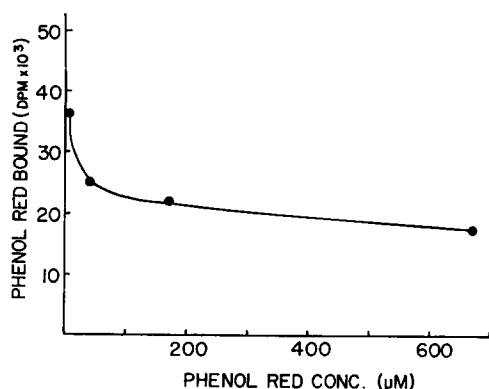


Fig. 3. The reversibility of phenol red binding. The binding of phenol red was initiated at a concentration of $0.01 \mu\text{M}$; after 15 min of incubation, 0.2 ml of Cross-Taggart buffer or various concentrations of unlabeled phenol red were added to the incubation mixture and reincubated for 15 min. Binding was determined as described in Materials and Methods section. Each point represents the mean of three experiments.

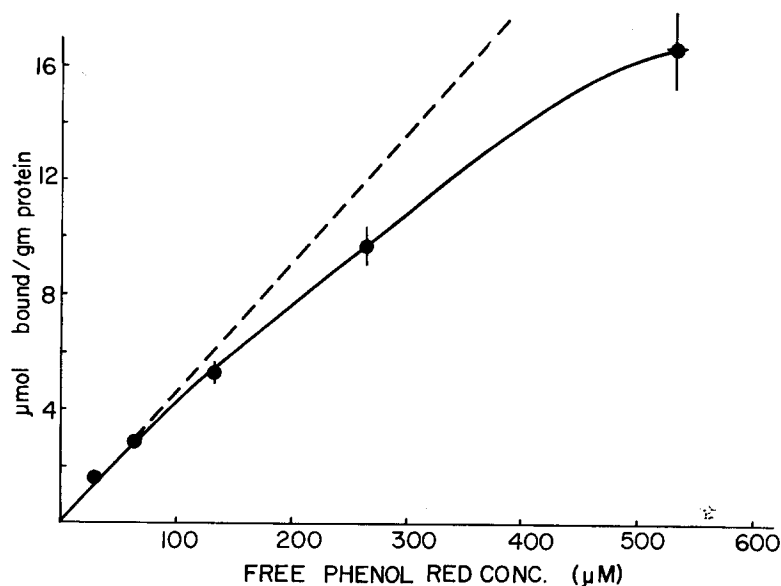


Fig. 4. The dependence of phenol red binding by renal cortical microsomes on the concentration of free phenol red. The dashed line represents a hypothetical linear relationship between the concentration of the dye and the binding of phenol red. The solid line indicates the actual binding of phenol red with increasing dye concentrations. Points represent means \pm S.E. ($n = 16$).

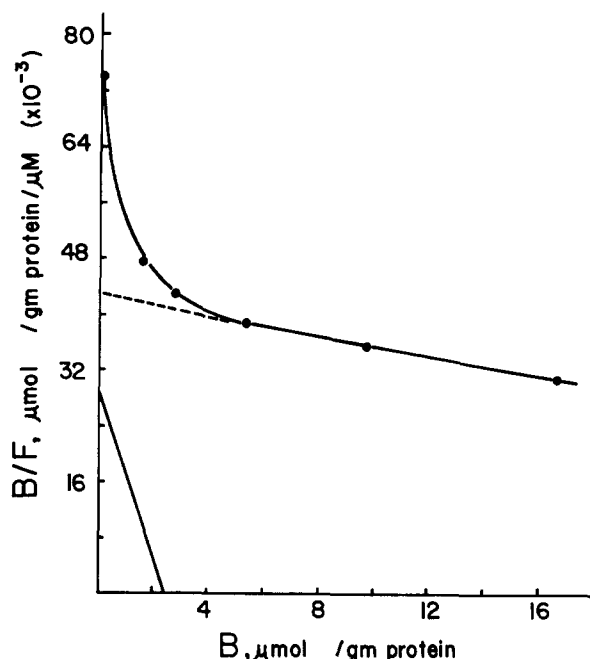


Fig. 5. Scatchard analysis of the binding of phenol red to renal cortical microsomes. The binding curve intersects the y-axis at a point equal to $(K_{a_1}n_1 + K_{a_2}n_2)$, where K_a is the association constant, n , the binding site concentration and 1 and 2 refer to the high and the low affinity binding sites, respectively [25, 26]. By extrapolating the slope of the low affinity population of binding sites back to zero on the y-intercept ($K_{a_2}n_2$), the association constant and binding site concentration can be calculated by subtraction. The corrected high affinity component is represented in the lower left hand corner. The high affinity binding site has a $K_{a_1} = 11.29 \cdot 10^3 \text{ M}^{-1}$ and $n_1 = 2.41 \text{ } \mu\text{mol bound/g protein}$. The low affinity population had a $K_{a_2} = 0.80 \cdot 10^3 \text{ M}^{-1}$ and $n_2 = 55.06 \text{ } \mu\text{mol of phenol red bound/g protein}$. Each point represents the mean of eight experiments.

bility; however, saturation was incomplete at free phenol red concentrations as high as $600 \text{ } \mu\text{M}$. Further increases in phenol red concentration were unobtainable due to the intense color of the medium which quenched greater than 99.5 % of the radioactive counts present in the scintillation fluid. Two distinct populations of binding sites for phenol red in the microsomal fraction could be identified by Scatchard analysis (Fig. 5) [18]. The high affinity, low capacity binding site had an association constant (K_{a_1}) equal to $11.29 \cdot 10^3 \text{ M}^{-1}$ and $2.41 \text{ } \mu\text{mol}$ of phenol red were bound per g of protein (n_1). A low affinity, high capacity binding component could be identified which had an association constant (K_{a_2}) of $0.80 \cdot 10^3 \text{ M}^{-1}$ and $55.06 \text{ } \mu\text{mol}$ of phenol red could be found per g of protein (n_2). The two classes of binding sites did not interact as is shown by the Hill plot (Fig. 6). A slope of 0.9 indicates that the binding sites are independent and no cooperativity exists between the binding sites.

Effects of competitive inhibitors on phenol red binding. Probenecid and 2,4-dinitrophenol, competitive inhibitors of phenol red secretion in mammals, were found to be competitive inhibitors of phenol red binding to renal cortical microsomes. Probenecid (0.32 mM) was found to competitively inhibit only the high affinity binding sites for phenol red (Fig. 7). The high affinity association constant decreased

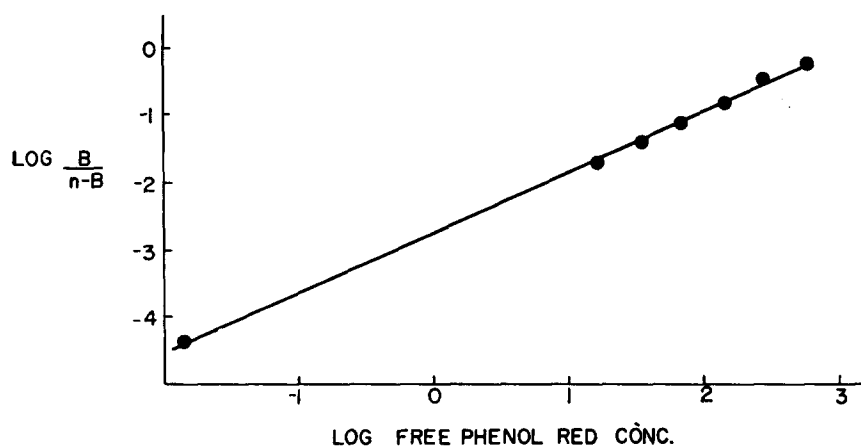


Fig. 6. Hill plot of phenol red binding. The slope = 0.9. The points represent the means of four experiments.

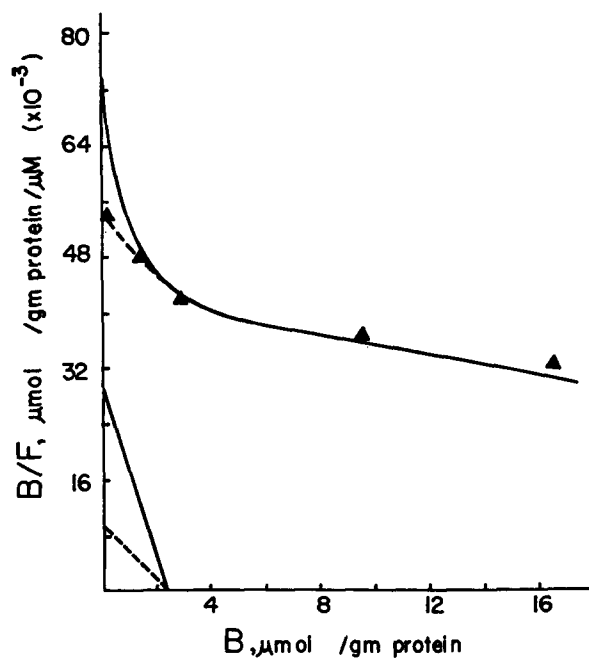


Fig. 7. Scatchard analysis of the effect of 0.32 mM probenecid on phenol red binding to the microsomal fraction. The solid line represents the control (from Fig. 5). The dashed lines and triangles represent phenol red binding in the presence of probenecid. In the control experiments, $K_{a1} = 11.29 \cdot 10^3 \text{ M}^{-1}$, $n_1 = 2.41$. In the presence of 0.32 mM probenecid, $K_{a1} = 4.61 \cdot 10^3 \text{ M}^{-1}$ ($P < 0.001$), $n_1 = 2.12$ ($P > 0.1$). Each triangle represents the mean of four experiments.

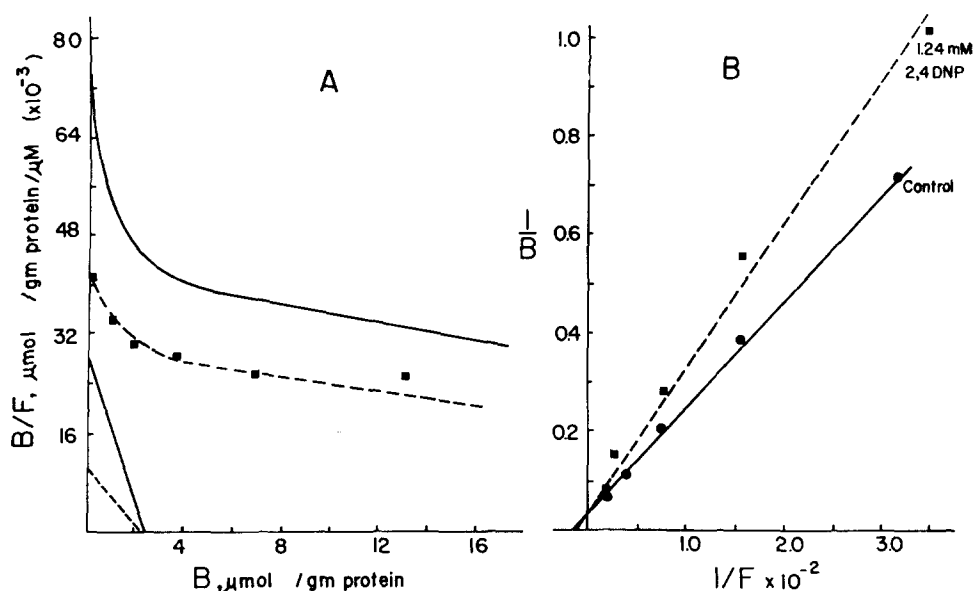


Fig. 8. (A) Scatchard analysis of the effect of 1.24 mM 2,4-dinitrophenol on phenol red binding. The solid line represents phenol red binding in the control (from Fig. 5): $K_{a1} = 11.29 \cdot 10^3 \text{ M}^{-1}$, $n_1 = 2.41$. The dashed lines and squares indicate phenol red binding in the presence of 2,4-dinitrophenol: $K_{a1} = 6.01 \cdot 10^3 \text{ M}^{-1}$ ($P < 0.001$), $n_1 = 2.20$ ($P > 0.1$). (B) Lineweaver-Burk analysis of the effects of 1.24 mM 2,4-dinitrophenol on phenol red binding to the low affinity binding sites. The symbols represent the means of four experiments.

from $11.29 \cdot 10^3$ to $4.61 \cdot 10^3 \text{ M}^{-1}$ in the presence of probenecid ($p < 0.001$). The binding site concentration did not change significantly ($p > 0.1$). This action of probenecid, decreasing the association constant but not altering the maximal binding site capacity, is consistent with the concept of probenecid acting as a competitive inhibitor of the high affinity binding population for phenol red.

The addition of 2,4-dinitrophenol (1.24 mM) to the incubation medium decreased phenol red binding in both the high and the low affinity binding populations (Fig. 8). Employing Scatchard analysis, the association constant of the high affinity sites decreased from $11.29 \cdot 10^3$ to $6.01 \cdot 10^3 \text{ M}^{-1}$ ($P < 0.001$), but the binding site concentration did not change in the presence of the inhibitor (Fig. 8A). The use of Lineweaver-Burk transformations [19] on the binding parameters places weight on the points of the low affinity population, and therefore, the action of 2,4-dinitrophenol on the low affinity binding sites was tested by Lineweaver-Burk analysis (Fig. 8B). 2,4-Dinitrophenol competitively inhibited phenol red binding in the low affinity binding population, and decreased the association constant without altering the binding site capacity.

Cationic requirement for phenol red binding. Phenol red binding was influenced significantly by the cationic composition of the incubation medium. Decreasing the sodium and potassium concentrations to 19 and 6.7 mequiv./l, respectively, decreased phenol red binding to both the high and the low affinity binding populations of the microsomal fraction (Figs. 9 and 10). Scatchard analysis demonstrated that the

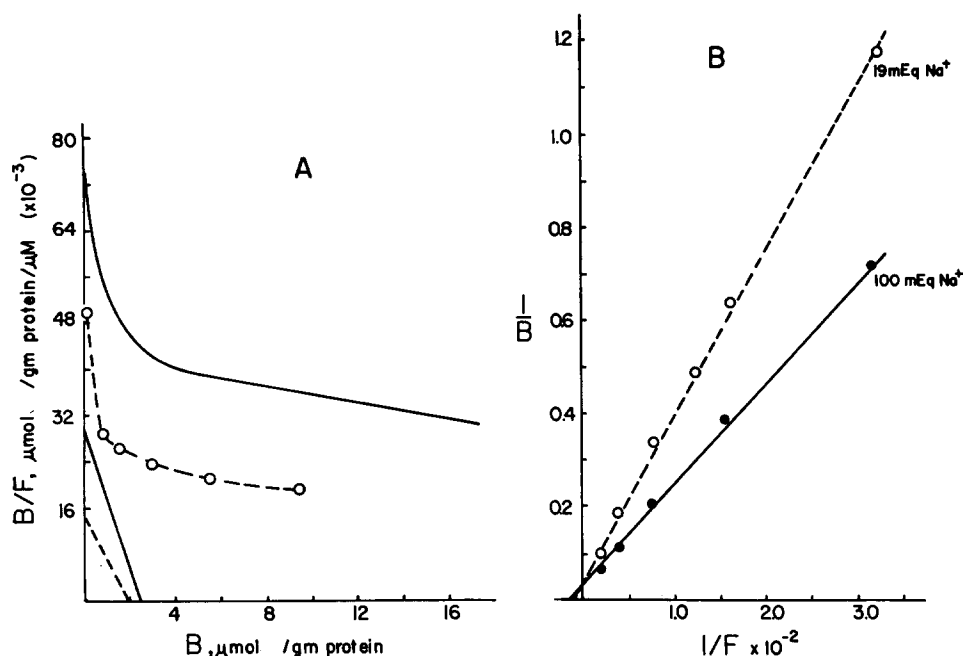


Fig. 9. (A) The binding of phenol red to renal microsomes in the medium containing 100 or 19 mequiv. Na^+ /l. The solid line represents phenol red binding in the control (from Fig. 5): $\text{Na}^+ = 100$ mequiv./l, $K_{a1} = 11.29 \cdot 10^3 \text{ M}^{-1}$, $n_1 = 2.41$. The dashed lines and open circles represent phenol red binding with $\text{Na}^+ = 19$ mequiv./l: $K_{a1} = 6.80 \cdot 10^3 \text{ M}^{-1}$ ($P < 0.01$), $n_1 = 1.84$ ($P > 0.1$). Each point is the mean of four experiments. (B) Lineweaver-Burk analysis of the effect of decreasing sodium concentration from 100 to 19 mequiv./l on phenol red binding. Each point is the mean of four experiments.

high affinity association constant was decreased from $11.29 \cdot 10^3$ to $6.80 \cdot 10^3 \text{ M}^{-1}$, when the sodium concentration was lowered from 100 to 19 mequiv./l ($p < 0.01$) (Fig. 9A). The binding site concentration also decreased from 2.41 to $1.84 \mu\text{mol}$ per g of protein ($p > 0.1$). The use of Lineweaver-Burk analysis indicated that decreasing the sodium concentration lowered the affinity of phenol red for the low affinity population of binding sites without changing the maximal binding capacity of the system (Fig. 9B).

Similar effects were seen by altering the potassium concentration of the incubation medium (Fig. 10A). Decreasing the potassium concentration from 40 to 6.7 mequiv./l decreased the association constant of the high affinity binding population from $11.29 \cdot 10^3$ to $7.44 \cdot 10^3 \text{ M}^{-1}$ ($P < 0.01$). The binding site concentration did not change with decreases in the potassium concentration. Lineweaver-Burk analysis indicated that decreasing potassium concentrations also decreased the affinity of the phenol red to the low capacity binding system without changing the binding site concentration (Fig. 10B).

Decreasing calcium concentrations from 1.5 to 0.25 mequiv./l did not alter the binding of phenol red to either the high or the low affinity binding populations.

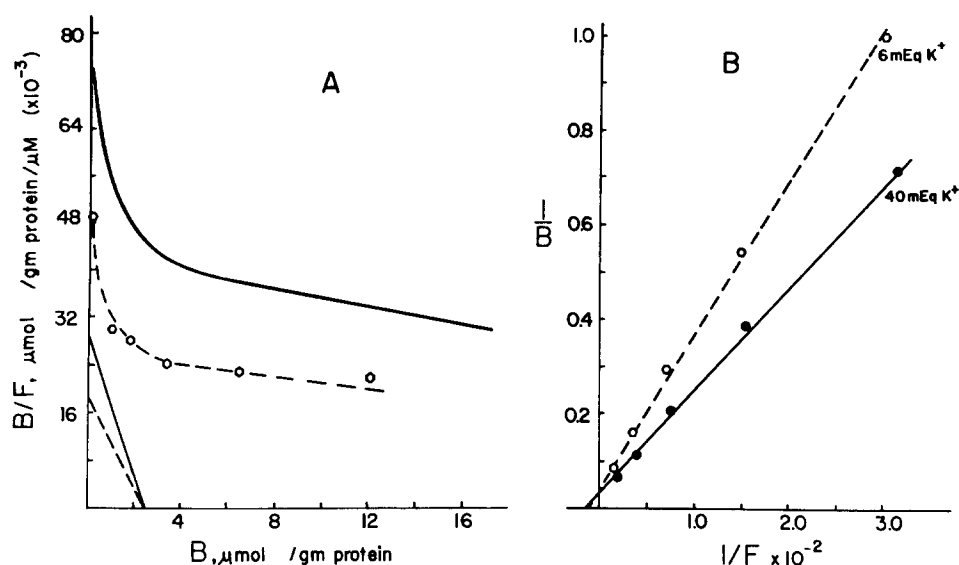


Fig. 10. Scatchard analysis of the effects of decreasing potassium concentrations from 40 to 6.7 mequiv./l on phenol red binding. The dashed lines and open circles indicate phenol red binding at 6.7 mequiv./l K^+ : $K_{a1} = 7.44 \cdot 10^3 \text{ M}^{-1}$, $n_1 = 2.41$. The solid line represents binding in the control (from Fig. 5): $K^+ = 40$ mequiv./l, $K_{a1} = 11.29 \cdot 10^3 \text{ M}^{-1}$ ($P < 0.01$), $n_1 = 2.41$. Each point is the mean of four experiments. (B) Lineweaver-Burk analysis of phenol red binding when potassium concentrations are decreased from 40 to 6.7 mequiv./l. Each point represents the mean of four experiments.

To test whether a specific $(\text{Na}^+ + \text{K}^+)\text{-ATPase}$ was implicated in phenol red binding to the microsomal fraction $8 \cdot 10^{-4} \text{ M}$ ouabain was added to the incubation medium. Phenol red binding to either the high or the low affinity binding populations was unaffected by the addition of ouabain.

DISCUSSION

In the present study, phenol red binding was inhibited significantly by probenecid, a powerful competitive inhibitor of phenol red transport, in only the microsomal fraction of the cell (Fig. 2). The concentration of inhibitor was 1000 times the concentration of phenol red, yet the decrease in total binding produced by probenecid was not as large as expected based on the magnitude of probenecid inhibition of phenol red transport seen in rabbit kidney slices by Park et al. [20]. However, probenecid decreased binding in only the high affinity, low capacity binding population and since the high affinity sites comprised a small percentage (4.2 %) of the total binding capacity for phenol red, the small decrease shown in total binding was not surprising.

Kinetics of microsomal binding. The association constant for the high affinity phenol red binding site was $1.13 \cdot 10^4 \text{ M}^{-1}$ which agrees well with calculated association constants for organic acid transport from other investigators. The association constant calculated from the work by Berndt [13] for probenecid binding to whole homogenates of rabbit renal cortex was $1.40 \cdot 10^5 \text{ M}^{-1}$. The association constant

calculated from the uptake of *p*-aminohippurate into basal-lateral membrane vesicles of rat kidney as reported by Berner and Kinne [21] was $1.85 \cdot 10^4 \text{ M}^{-1}$ and by Park et al. [20] from phenol red uptake in rabbit kidney slices, $0.6 \cdot 10^4 \text{ M}^{-1}$ ($1/K_m$).

The present data show no cooperative effects for the binding of phenol red to the microsomal material (Fig. 6). Holohan et al. [11] recently suggested that a positive cooperative effect existed for the binding of *p*-aminohippurate to dog cortical particulate fractions. There is no explanation for this discrepancy of data; however, no reports have been published suggesting cooperative effects for the transport of organic acids at low concentrations.

Effects of competitive inhibitors and cations. Probenecid and 2,4-dinitrophenol, competitors for phenol red secretion, were found to be competitive inhibitors of phenol red binding to the high affinity binding sites (Figs. 7 and 8). The low affinity binding sites were additionally competitively inhibited by 2,4-dinitrophenol. It is attractive to speculate that the binding of phenol red to the high affinity binding population of the rabbit renal microsomal fraction represented the initial reaction in active transport of the dye to the basal-lateral membranes of the renal proximal tubule and that phenol red binding to the low affinity class of binding sites represented the binding of the dye to intracellular ligands. Kinetic analyses from previous experimental data give credence to such a hypothesis. Inhibitors such as probenecid appear to act competitively only with the carrier-substrate complex, blocking entry into the cell, whereas, 2,4-dinitrophenol and Diodrast have been postulated to not only inhibit the entry of *p*-aminohippurate into the cell but competitively displace it from bound intracellular pools [7-9]. Although the data presented here are consistent with this proposed scheme, it is clear that the hypothesis requires further testing.

Decreasing the sodium and potassium concentrations of the incubation medium decreased the binding affinity of phenol red to the microsomal fraction at both the high and the low affinity binding sites. This is in accordance with the findings of Hoshi and Hayashi [22], who demonstrated that decreases in the sodium concentration of the bathing medium decreased phenol red uptake into goldfish kidney slices by increasing the K_m of the transport system without changing the maximal transport rate. These authors also demonstrated decreased phenol red uptake at potassium concentrations less than 10 mequiv./l, maximum enhancement of phenol red was found at potassium concentrations between 10 and 30 mequiv./l. This is in contrast to the data of Foulkes and Miller [23], who found maximum *p*-aminohippurate uptake into rabbit cortical slices at 2 mequiv./l potassium in the bathing medium. Also, Gerencser et al. [24] have demonstrated that a decrease in the sodium concentration of the medium decreased the maximal velocity of the transport reaction yet had no effect on the affinity of the carrier for *p*-aminohippurate, suggesting a separate carrier system for phenol red and a common phenol red-*p*-aminohippurate carrier system may be functioning.

The question of whether the binding of phenol red to the microsomal membranes represents the specific binding of the dye to receptor sites on the basal-lateral membrane or reflects specific binding to the membrane subsequent to uptake into membrane bound vesicles is complex and difficult to solve. In initial binding studies, identical binding parameters were obtained with three different binding methods: equilibrium dialysis, ultrafiltration and centrifugation. The time allowed for in-

cubation between the membranes and phenol red would have allowed for a steady state to be established between binding and vesicular uptake, thus, kinetically, the high affinity Scatchard component would still reflect the binding behavior of phenol red and, in this case, the low affinity binding class might represent the transport component. Yet, we believe the difference between the effects of probenecid and 2,4-dinitrophenol on the kinetics of phenol red binding indicate that we are studying a true binding system.

ACKNOWLEDGEMENTS

The authors gratefully acknowledge the splendid technical assistance of Sandra Yamamoto. We also thank Benjamin Respicio for the skilful construction of our experimental apparatus. This investigation was supported in part by a Grant-in-Aid from the American Heart Association (72-633) and in part by the Hawaii Heart Association.

REFERENCES

- 1 Forster, R. P. and Copenhaver, Jr., J. H. (1956) *Am. J. Physiol.* 186, 167-171
- 2 Foulkes, E. C. and Miller, B. F. (1955) *Am. J. Physiol.* 196, 83-85
- 3 Huang, K. C. and Lin, D. S. T. (1965) *Am. J. Physiol.* 208, 391-396
- 4 Berndt, W. O. (1966) *Biochem. Pharmacol.* 15, 1947-1956
- 5 Copenhaver, Jr., J. H. and Forster, R. P. (1958) *Am. J. Physiol.* 195, 327-330
- 6 Farah, A., Frazer, M. and Stoffel, M. (1963) *J. Pharm. Exp. Ther.* 139, 120-128
- 7 Foulkes, E. C. and Miller, B. F. (1959) *Am. J. Physiol.* 196, 86-92
- 8 Ross, C. R. and Farah, A. (1966) *J. Pharm. Exp. Ther.* 151, 159-161
- 9 Sheikh, M. I. and Moller, J. V. (1970) *Biochim. Biophys. Acta* 196, 305-319
- 10 Welch, L. T. and Bush, M. T. (1970) *Am. J. Physiol.* 218, 1751-1756
- 11 Holohan, P. D., Pessah, N. I. and Ross, C. R. (1975) *J. Pharm. Exp. Ther.* 195, 22-33
- 12 Sheikh, M. I. (1972) *J. Physiol. Lond.* 227, 565-590
- 13 Berndt, W. O. (1967) *Proc. Soc. Exp. Biol. Med.* 126, 123-126
- 14 Cross, R. J. and Taggart, J. V. (1950) *Am. J. Physiol.* 161, 181-190
- 15 de Duve, C., Pressman, B. C., Gianetto, R., Wattiaux, R. and Appelmans, F. (1955) *Biochem. J.* 60, 604-617
- 16 Fiske, C. H. and SubbaRow, Y. (1925) *J. Biol. Chem.* 66, 375-400
- 17 Lowry, O. H., Rosebrough, N. J., Farr, A. L. and Randall, R. J. (1951) *J. Biol. Chem.* 193, 265-275
- 18 Scatchard, G. (1949) *Ann. N.Y. Acad. Sci.* 51, 660-672
- 19 Lineweaver, H. and Burk, D. (1934) *J. Am. Chem. Soc.* 56, 658-666
- 20 Park, Y. S., Yoo, H. S. and Hong, S. K. (1971) *Am. J. Physiol.* 220, 95-99
- 21 Berner, W. and Kinne, R. (1976) *Pflügers Arch.* 361, 269-277
- 22 Hoshi, T. and Hayashi, H. (1970) *Jap. J. Physiol.* 20, 683-696
- 23 Foulkes, E. C. and Miller, B. F. (1961) in *Membrane Transport and Metabolism* (Kleinzeller, A. and Kotyk, A., eds.), pp. 559-565, Academic Press, London
- 24 Gerencser, G. A., Park, Y. S. and Hong, S. K. (1973) *Proc. Soc. Exp. Biol. Med.* 144, 440-444
- 25 Feldman, H. A. (1972) *Anal. Biochem.* 48, 317-338
- 26 Rodbard, D. (1973) in *Advances in Experimental Medicine and Biology* (O'Malley, B. W. and Means, A. R., eds.), Vol. 36, pp. 289-326, Plenum, New York